Dynamic Simulation of Maglev Water Pump on A Moving Base by Using Multibody Dynamics Method

Yanhui MA [a,b], Yixin SU [a,b], Yichen YAO [a,b,c], Suyuan YU [a,b]

[a] Center for Combustion Energy, Tsinghua University, 100084 Beijing, China, suyuan@tsinghua.edu.cn
[b] Department of Energy and Power Engineering, Tsinghua University, 100084 Beijing, China
[c] School of Energy and Environment, Southeast University, 210096 Nanjing, China

Abstract—**As one of the key components of a rotating machinery, the bearing has a significant effect on the dynamic response of the system. Compared with traditional mechanical bearings, the magnetic bearing has many advantages such as no contact and friction, no need of lubrication, no wear, low noise, high rotational speed, etc. Therefore, the magnetic bearing is an ideal support for rotating machinery, i.e. a maglev water pump. During the modeling and simulation the magnetic bearing, it is usually simplified as a spring-dampers with equivalent stiffness and damping, which ignore the dynamic characteristics of the magnetic bearing. Besides, the study of simulation mainly focuses on the vibration reduction of the rotor or the vibration transfer to the base, while little was known about the dynamic response of the maglev machinery system on a moving base. In this paper, a time-domain rigid-flexible coupling simulation model of a maglev water pump on a moving base is established by using multibody dynamics method. In this model, the flexible rotor is simplified as several discrete rigid parts connected with massless beam force and the control system of the magnetic bearing with PID controller is realized by utilizing state space equations. Then the dynamic response of the maglev water pump on a pitching and rolling base was obtained based on the established model.**

I. INTRODUCTION

Vibrations and noise are unavoidable when the rotating machinery running, which cause many problem, for example, the vibration will reduce the mechanical efficiency and service life, the excessive noise can affect operator's health. Therefore, decreasing the vibration and noise of the rotating machinery is a vital requirement.

Bearing, as the indispensable key components for rotating machinery, is not only the major vibration excitation source, but also the main vibration transmission path, therefore its mechanical characteristic has a significant influence on the vibration generation and transmission of rotating machinery.

Traditional mechanical bearing is widely used in rotating machinery, however, mechanical bearing produces large rotational resistance and cause vibration and noise because of the contact and friction, so designing and selecting a suitable bearing has become a significant work in the design of rotating machinery.

Active magnetic bearing is an ideal support component, in which make the rotor suspend stably in space by a magnetic force with feedback control. Because that there is no contact and friction between the rotor and bearing, and it has some advantages in comparison with conventional mechanical bearings, e.g. no need of lubrication, no wear, low noise, high rotational speed. Therefore, magnetic bearing has a wide application prospect in rotating machinery.

In the past research, during the mechanics simulation of magnetic bearing, the magnetic bearing was substituted by spring-dampers with equivalent stiffness and damping[1, 2], which is often leads to inaccurate results due to ignoring the influence of the dynamic characteristics of magnetic bearing[3].

As shown in Fig.1, a maglev water pump normally consists of a rotor, a stator, a pump, a five-degrees of freedom magnetic system which is composed of two radial and one axial magnetic. The control system of the magnetci bearing comprises controller, sensor and power amplifier. The mechanical part of the maglev water pump is a typical complex multibody dynamics system, therefore, multibody dynamics method is used to establish the dynamics simulation model of the maglev water pump in this paper, .and the control system of the magnetic bearing with PID controller is described by utilizing state space equations.

II. DYNAMIC MODEL

In multibody dynamics method, the mechanical system is divided into several rigid parts or flexible parts according to the mechanical behaviors, then the mechanical system can be simulated by applying joints, forces or contact between each parts. Compared with finite element method, multibody dynamics method has higher accuracy and speed with fewer degrees of freedom so that it is widely used to simulate the kinematics and dynamics of complex mechanical system.In this section, the dynamics equations of the system will be given, with particular focus on the rotor and control system of the magnetic bearing.

A. Rigid-Flexible coupling model of rotor

To simulate the flexible characteristics of the rotor, the rotor was discretized into as a series of lumped masses connected with each other by massless flexible beams, as shown in Fig 1. The mass and inertia of the rotor can be described by these lumped masses, meanwhile, the elastic and damping characteristics can be simulated by the connected massless beam segments.

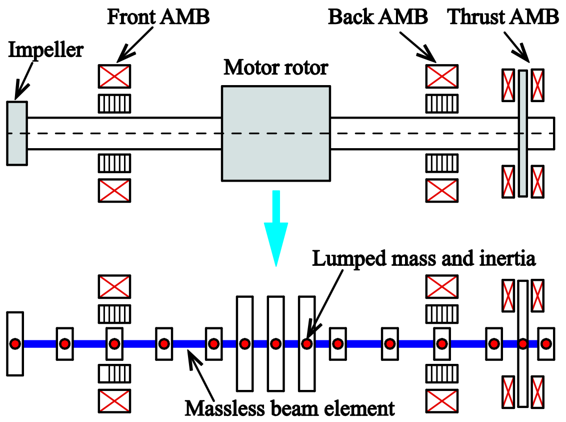

Figure 1. Rigid-flexible couping model of maglev water pump

Taking the center position coordinates $\mathbf{r}_b=[x,y,z]^{\mathrm{T}}$ in the global coordinate system and the normalized quaternion $\boldsymbol{\lambda}_b=[\lambda_0,\lambda_1,\lambda_2,\lambda_3]^{\mathrm{T}}$ based on Euler's rotation theorem as the generalized coordinate of rigid body:

$$\mathbf{q}=[\mathbf{r}_b,\boldsymbol{\lambda}_b]^{\mathrm{T}} \tag{1}$$

And the normalized quaternions $\boldsymbol{\lambda}_b$ satisfies the following constraints:

$$\Phi_\lambda=\boldsymbol{\lambda}_b^{\mathrm{T}}\boldsymbol{\lambda}_b=1 \tag{2}$$

Assume that there are n_c constraints in the system, the constraint equations can be expressed as:

$$\Phi_k(\mathbf{q}_1,\mathbf{q}_2,\ldots,\mathbf{q}_n,t)=0 \qquad k=1,2,\ldots,n_c \tag{3}$$

Apply Lagrange equation of the first kind, the governing equations of the rigid bodies can be obtained as[4]

$$\mathbf{M}_i\ddot{\mathbf{q}}_i+\mathbf{Q}_i-\mathbf{P}_i+\sum_{k=1}^{n_c}\boldsymbol{\Phi}_{k,q_i}^{\mathrm{T}}\mu_i=0,\quad i=1,2,\ldots,n_b \tag{4}$$

And

$$\mathbf{M}_i=\begin{bmatrix}\mathrm{m}_i\mathbf{I} & 0\\ 0 & 4\mathbf{G}^T\mathbf{J}_i\mathbf{G}\end{bmatrix}$$

$$\mathbf{G}_i=\begin{bmatrix}-\lambda_1^i & \lambda_0^i & \lambda_3^i & -\lambda_2^i\\ -\lambda_2^i & -\lambda_3^i & \lambda_0^i & \lambda_1^i\\ -\lambda_3^i & \lambda_2^i & -\lambda_1^i & \lambda_0^i\end{bmatrix}$$

$$\mathbf{Q}_i=(\mathbf{V}_i-\frac{1}{2}\mathbf{V}_i^T)\dot{\mathbf{q}}_i$$

$$\mathbf{V}_i=\frac{\partial(\mathbf{M}_i\dot{\mathbf{q}}_i)}{\partial\mathbf{q}_i}$$

Where $\mathbf{M}_i$ is the mass matrix, $\boldsymbol{\Phi}_{k,q_i}^{\mathrm{T}}$ is Jacobian matrix of the constraint function. μ_i is the corresponding Lagrange multiplier. $\mathbf{Q}_i$ is generalized force vector relates to the generalized velocity. $\mathbf{P}_i$ is the generalized external forces vector.

For the rotor, the generalized external forces include the generalized force $\mathbf{P}_i^g$ of the gravity F_i^g and the generalized force $\mathbf{P}_i^e$ of the elastic beams.

Based on the principle of virtual work, the generalized force $\mathbf{P}_i^g$ of the gravity can be written as:

$$\mathbf{P}_i^g=\begin{Bmatrix}F_i^g\\ 0_{4\times1}\end{Bmatrix} \tag{5}$$

In this paper, the stiffness matrix of the massless beam obtained according to the Timoshenko beam theory and the damping is decoupled as Rayleigh damping. Then the linear translational and linear rotational force acted on the Mass I by Mass J is depends on the displacement $\Delta\mathbf{r}$ and rotation $\Delta\boldsymbol{\theta}$ and velocity of Mass I relative to Mass J:

$$\begin{Bmatrix}\mathbf{F}_i^b\\ \mathbf{T}_i^b\end{Bmatrix}=\mathbf{K}\begin{Bmatrix}\Delta\mathbf{r}\\ \Delta\boldsymbol{\theta}\end{Bmatrix}+\mathbf{C}\begin{Bmatrix}\Delta\dot{\mathbf{r}}\\ \Delta\dot{\boldsymbol{\theta}}\end{Bmatrix} \tag{6}$$

Where $\mathbf{K}$ and $\mathbf{C}$ is the stiffness and damping matrix.

Based on the relationship between the variation of quaternions and virtual rotation, the virtual work of the beam force is:

$$\begin{aligned}\delta W&=\delta\mathbf{r}^{\mathrm{T}}\mathbf{F}_i^b+\delta\boldsymbol{\theta}^{\mathrm{T}}\boldsymbol{\tau}_i^b\\ &=(\delta\mathbf{r}_i^{\mathrm{T}}+\delta\boldsymbol{\lambda}_i^{\mathrm{T}}2\mathbf{G}_i^{\mathrm{T}}\tilde{\mathbf{s}}_i)\mathbf{F}_i^b+2\delta\boldsymbol{\lambda}_i^{\mathrm{T}}\mathbf{G}_i^{\mathrm{T}}\boldsymbol{\tau}_i^b\end{aligned} \tag{7}$$

Then the generalized external force acted on Mass I can be written as:

$$\mathbf{P}_i^b=\begin{Bmatrix}\mathbf{F}_i^b\\ 2\mathbf{G}_i^{\mathrm{T}}(\mathbf{T}_i^b+\tilde{\mathbf{s}}_i\mathbf{F}_i^b)\end{Bmatrix} \tag{8}$$

Where $\mathbf{G}_i^{\mathrm{T}}$ is the force-mapping matrix. $\tilde{\mathbf{s}}_i$ is the vector of the application point of force $\mathbf{F}_i^b$ in the body frame of Mass I. Similarly, the generalized external force acted on Mass J is:

$$\mathbf{P}_j^b=\begin{Bmatrix}-\mathbf{F}_i^b\\ -2\mathbf{G}_j^{\mathrm{T}}(\boldsymbol{\tau}_i^b+\tilde{\mathbf{s}}_j\mathbf{F}_i^b+\tilde{\mathbf{s}}_j^i\mathbf{F}_i^b)\end{Bmatrix} \tag{9}$$

B. Mechanics simulation of magnetic bearing

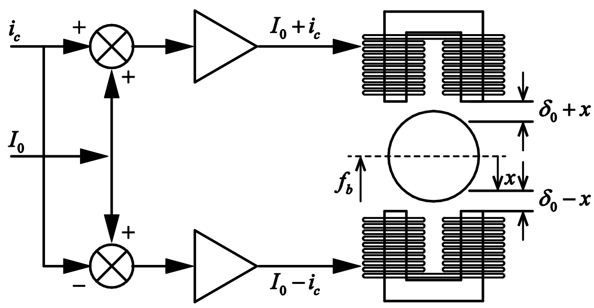

Figure 2. Principle of magnetic bearing

Take the single degree of freedom magnetic bearing model shown in Fig. 2 as an example, the electromagnetic force of magnetic bearing with differential electromagnetic structure is:

$$f_b=\frac{\mu_0AN^2}{4}\left[\frac{(I_0+i_0+i_c)^2}{(\delta_0+x)^2}-\frac{(I_0-i_0-i_c)^2}{(\delta_0-x)^2}\right] \tag{10}$$

Where $4\pi\times10^{-7}\,\mathrm{N/A^2}$ is the permeability of vacuum, A is the cross-section area of magnetic pole, N is number of windings in each magnetic pole, I_0 is the bias current, i_0 is static bias current that produce electromagnetic force to overcome gravity at equilibrium position, i_c is the control current, δ_0 is the air gap of magnetic bearing. Linearizing Eq.(10) at the equilibration position($x=0, i_c=0$):

$$\begin{aligned} f_b(x,i_c) &= f_b(0,0) + \frac{\mu_0 A N^2 I_0}{\delta_0^2} i_c - \frac{\mu_0 A N^2 (I_0+i_0)^2}{\delta_0^3} x \\ &= f_b(0,0) + k_i i_c - k_x x \end{aligned} \tag{11}$$

Where k_i and k_x are the current stiffness coefficient and displacement stiffness coefficient respectively.

Since $(i_0/I_0)^2 \ll 1$, k_x can be simplify as:

$$k_x = \frac{\mu_0 A N^2 I_0^2}{\delta_0^3} \tag{12}$$

Different control strategies are applied to make the rotor suspend stably for the magnetic bearing, such as PID control, robust control and adaptive control. The most common is PID control because of its conception is clear and arithmetic is simple. The whole control system consists of PID controller, sensor and power amplifier.

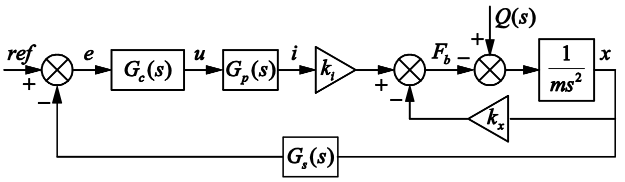

Figure 3. Block diagram of a magnetic bearing with PID controller

The block diagram is shown in Fig.3. The transfer functions of the PID controller $G_c(s)$, sensor $G_s(s)$ and power amplifier $G_p(s)$ are:

$$\begin{aligned} G_c(s) &= K_p + \frac{K_i}{1+T_i s} + \frac{K_d s}{1+T_d s} \\ G_s(s) &= \frac{A_s}{1+T_s s} \\ G_p(s) &= \frac{A_a}{1+T_a s} \end{aligned} \tag{13}$$

Where K_p, K_i, K_d are the proportional, integral and derivative coefficients, respectively. T_i, T_d are the integral and derivative time parameters. A_s, T_s are the sensor gain and time parameter. A_p, T_p are the power amplifier gain and time parameter. Ignoring the influence of T_s and T_p, then the equivalent stiffness and damping coefficient of the magnetic bearing are[5]:

$$\begin{aligned} k_b &= k_i A_s A_a \left(K_p + \frac{K_i}{1+T_i^2\omega^2} + \frac{K_d T_d \omega^2}{1+T_d^2\omega^2} \right) - k_x \\ c_b &= k_i A_s A_a \left(\frac{K_d}{1+T_d^2\omega^2} - \frac{K_i T_i}{1+T_i^2\omega^2} \right) \end{aligned} \tag{14}$$

Where ω is the controller frequency and usually replaced by rotor rotating frequency, which is often leads to inaccurate results due to ignoring the influence of the dynamic characteristics of magnetic bearing.

In this paper, the state space equations were used to describe the transfer function of the controller:

$$\begin{cases} \dot{\mathbf{x}} = \mathbf{A}\mathbf{x}(t) + \mathbf{B}\mathbf{u}(t) \\ \mathbf{y} = \mathbf{C}\mathbf{x}(t) + \mathbf{D}\mathbf{u}(t) \end{cases} \tag{15}$$

Where $\mathbf{A}$ is the state matrix, $\mathbf{B}$ is the input matrix, is $\mathbf{C}$ the output matrix, $\mathbf{D}$ is the feedthrough matrix, $\mathbf{x}$ is state vector, $\mathbf{y}$ is the output vector, $\mathbf{u}$ is the control vector.

The transfer function of magnetic bearing with SISO control system can be written as:

$$G(s) = \frac{b_m s^m + b_{m-1} s^{m-1} + \cdots b_1 s + b_0}{a_n s^n + a_{n-1} s^{n-1} + \cdots a_1 s + a_0} \tag{16}$$

The state vector can be set as the displacement of the rotor and its derivatives:

$$\mathbf{x} = [q, \dot{q}, \cdots q^{(n-1)}]^{\mathrm{T}} \tag{17}$$

Then the matrix expressions of the state space equations is[6]:

$$\begin{aligned} \mathbf{A} &= \begin{bmatrix} 0 & 1 & 0 & \cdots & 0 \\ 0 & 0 & 1 & \cdots & 0 \\ \vdots & \vdots & \vdots & \ddots & \vdots \\ 0 & 0 & 0 & \cdots & 1 \\ a_0 & a_1 & a_2 & \cdots & a_n \end{bmatrix}_{n\times n} \\ \mathbf{B} &= [0 \quad 0 \quad 0 \quad \cdots \quad 1]^{\mathrm{T}} \\ \mathbf{C} &= [b_0 \quad b_1 \quad \cdots \quad b_m \quad 0 \quad \cdots \quad 0] \\ \mathbf{D} &= 0 \end{aligned} \tag{18}$$

Similar to the generalized external force expressions of beam force, the generalized external force acted on Mass I (on the rotor) and Mass J (on the stator) can be written as:

$$\begin{aligned} \mathbf{P}_i^{mb} &= \begin{Bmatrix} \mathbf{F}_i^{mb} \\ 2\mathbf{G}_i^{\mathrm{T}} \tilde{\mathbf{s}}_i \mathbf{F}_i^{mb} \end{Bmatrix} \\ \mathbf{P}_j^{mb} &= \begin{Bmatrix} -\mathbf{F}_i^{mb} \\ -2\mathbf{G}_j^{\mathrm{T}} (\tilde{\mathbf{s}}_j \mathbf{F}_i^{mb} + \tilde{\mathbf{s}}_j^{i} \mathbf{F}_i^{mb}) \end{Bmatrix} \end{aligned} \tag{19}$$

C. Governing equations of the system

The governing equations of the system are obtained by combining Eq.(4) and Eq.(15):

$$\begin{cases} \mathbf{M}\ddot{\mathbf{q}} + \mathbf{C}_{\mathbf{q}}^{\mathrm{T}} \boldsymbol{\mu} = \mathbf{Q}(\mathbf{q}, \dot{\mathbf{q}}, t) \\ \mathbf{C}(\mathbf{q}, t) = 0 \\ \dot{\mathbf{x}} = \mathbf{A}\mathbf{x}(t) + \mathbf{B}\mathbf{u}(t) \\ \mathbf{y} = \mathbf{C}\mathbf{x}(t) + \mathbf{D}\mathbf{u}(t) \end{cases} \tag{20}$$

The solution scheme was shown in Fig.4. The governing equation form a set of differentialtion and algebraic equations, which can be solved by the implicit backward differentiation formula (BDF) method, and detailed solution scheme can be found in literature [6] and [7]. And the multibody dynamics simulation model of a maglev water pump was shown in Fig.5.

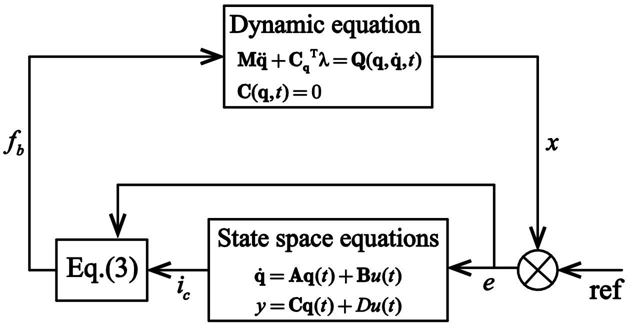

Figure 4. Solution scheme of the governing equation

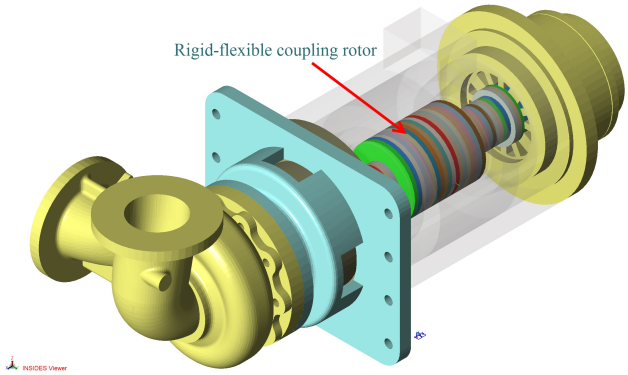

Figure 5. Multibody dynamics model of Maglev Water Pump

III. VALIDATION OF SYSTEM SIMULATION MODEL

A. gyroscopic force of the rotor

As shown in Fig.6, a circular-section rotating beam supported at the left end and free at the right end undergoes an impact force at the free end. According to literature [8] and [9], if the rotate angular speed is smaller than its first bending frequency(7.1 cycle/s), the vibration of the free end will attenuate because of the damping, and if it is larger than this speed, the vibration of the free end will produce a limit cycle under the effects of the gyroscopic effect. The simulation results shown in Fig.7 and Fig.8 indicate that the established rigid-flexible coupling rotor model can accurately simulate the dynamic characteristics of the rotor.

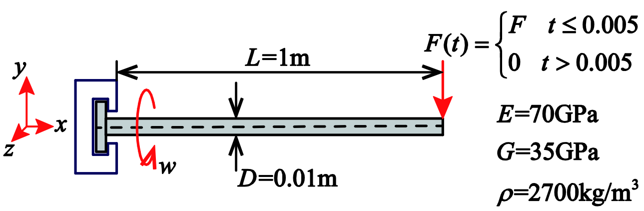

Figure 6. Rotation beam undergoes an impact force

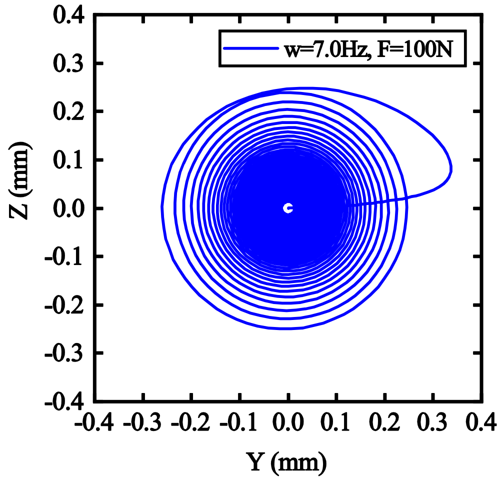

Figure 7. Trajectory of the free end when the rotating speed 7.0 cycle/s

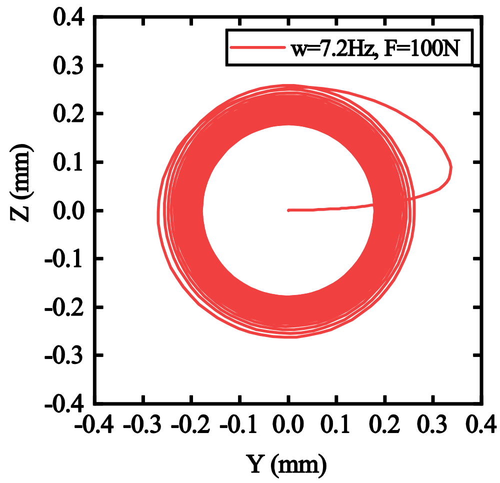

Figure 8. Trajectory of the free end when the rotating speed 7.2 cycle/s

B. Simulation verification of the magnetic bearing

In this section, the accuracy verification of the magnetic bearing with PID controller was carried out. A single degree of freedom (SDOF) magnetic bearing system shown in Fig.2 was established. Assuming the excitation acted on rotor is:

$$f(t)=100\sum_{i=1}^{3}\sin(2\pi f_i+\varphi_i) \tag{21}$$

And $f_1=10,\varphi_1=-\pi/6, f_2=50,\varphi_2=0, f_3=100,\varphi_3=\pi/6$.

Because the excitation has different frequency components, the equivalent stiffness and damping coefficient of the magnetic bearing is obtained as setting ω=50Hz, the parameters of the magnetic bearing is shown in Tab.1. According to Equ.(14), the equivalent stiffness and damping coefficient are 5.779 $\times 10^6$ N/m and 1.359 $\times 10^4$ N/ms^{-1}, respectively. To sufficient verify the correctness of the proposed model, A same simulation model was established by Simulink, the simulation block diagram was shown in Fig.9.

Table 1. Parameters of SDOF magnetic bearing

Parameters	Value
Mass of rotor	50 kg
Proportional coefficient	0.25
Integral coefficient	5
Integral time	1.5915
Derivative coefficient	0.001
Derivative time	0.0016
Displacement stiffness coefficient, k_x	8.9×10^5 N/m
Current stiffness coefficient, k_i	133 N/A
Sensor gain, A_s	3.33×10^4 V/m
Power amplifier gain, A_a	4 A/V

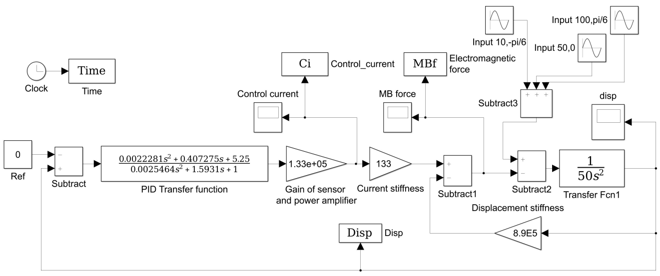

Figure 9. Controller system by Simulink

The comparison of simulation results of these three methods was shown in Fig.10. It is found that the simulation results obtained by the method proposed in this paper is entirely consistent with Simulink and is significant different with equivalent stiffness and damping model. It is because that the equivalent stiffness and damping of the magnetic bearing is connected with ω, In practical engineering, ω is a set of a number of frequency, therefore, using rotor rotating speed to substitute ω can cause a certain calculation errors.

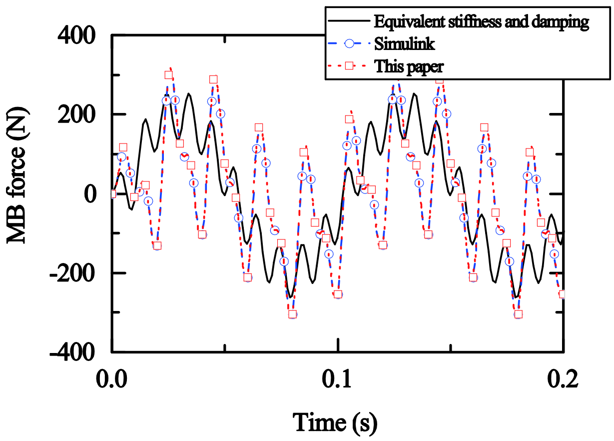

Figure 10. Comparison of simulation results of different models

IV. Dynamic Simulation of Maglev Water Pump on a Moving Base

A. Time-domain motion of the base

Currently, during the design and development process, it is often assumed that the base is fixed, which is reasonable in most cases, but when the base is moving, the inertial force and moment produced by the movement of the base motion will influence the dynamic response of the system. In this section, the harmonic displacement excitation of the base is considered to research this influence and evaluate the safety of the maglev water pump. The harmonic displacement excitations for the maglev water pump on a pitching or rolling base were assumed as:

$$x(t) = D\sin 2\pi ft \tag{22}$$

Where $D=\dfrac{\pi}{6}$ and $f=\dfrac{1}{3}$ are the angle amplitude and the frequency of the rolling or swing, respectively.

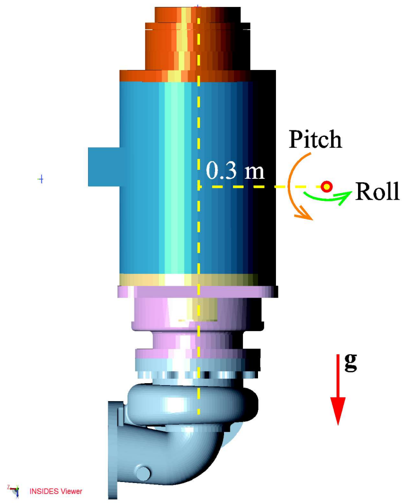

Figure 11. Controller system by Simulink

The rotor residual unbalance is one of the main excitation that cause the vibration of the system, the force caused by the unbalanced mass of rotor is applied on the mass center of rotor as excitation. Moreover, the Maglev Water Pump was suspended on the base through four flexible BE-120 supports that simplified as spring-damper with equivalent stiffness and damping.

B. Result and Discussion

Fig.12 shows the relative motion comparison of the front and back magnetic bearings between the maglev with fixed and moving base under harmonic displacement excitation. From the results, it can be found that the movement of the base results in an increase in the maximum relative displacement of the rotor. Compared with the rolling motion, the maximum relative displaceent under pitching motion is larger than fixed base because that the relative velocity between the rotor and two magnetic bearing is larger when the base start pitching movement, which increasing the contact risk between the rotor and magnetich bearing.

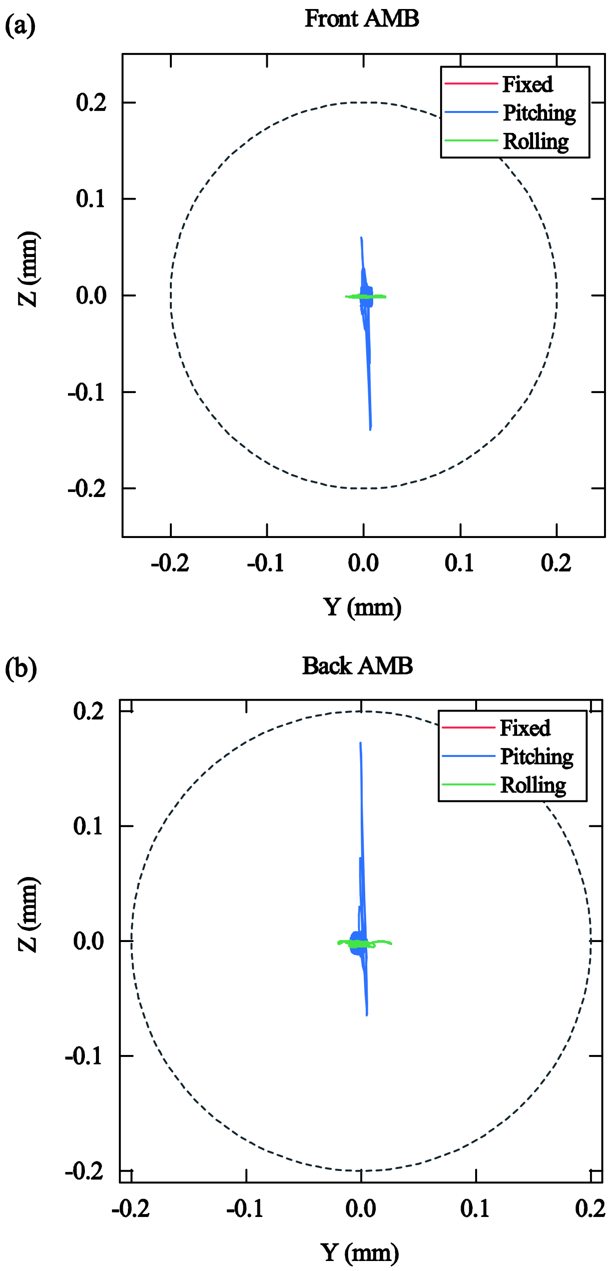

Figure 12. Relative motion comparison of the front and back AMBs.

V. CONLUSION

A rigid-flexible coupling simulation model of maglev water pump is established by using multibody dynamics method.

In this model, the flexible rotor is simplified as several discrete rigid parts connected with massless beam force; the control system of the magnetic bearing with PID controller is described by state space equations to properly simulation the dynamic characteristics of the control system and the nonlinear electromagnetic force of the magnetic bearing.

Then the dynamics behaviors of a maglev water pump suspended on a moving base were obtained based on this simulation model. It is found that the maximum relative displacement under pitching motion is larger than rolling motion. Therefore, when the pump needs to be mounted on a moving base, it is necessary to consider the influence of the base motion, especially pitching motion.

The simulation method proposed in this paper provides an effective simulation method for the dynamics simulation and design of other types of rotating machinery with magnetic bearing.

VI. ACKNOWLEDGMENTS

The authors thank the support and cooperation of the laboratory of multibody dynamics, Tsinghua University. The multibody dynamics simulation software INSIDES, developed by the laboratory members Prof. Gexue Ren, Zhihua Zhao and Dr. Jiawei He, provides a great help to establish the model of maglev water pump.

REFERENCES

[1] Jin C, Xu Y, Zhou J, et al. Active Magnetic Bearings Stiffness and Damping Identification from Frequency Characteristics of Control System[J]. Shock and Vibration,2016,(2016-1-10), 2016, 2016:1-8.

[2] Jiang K, Zhu C, Chen L, et al. Multi-DOF rotor model based measurement of stiffness and damping for active magnetic bearing using multi-frequency excitation[J]. Mechanical Systems & Signal Processing, 2015, 60-61:358-374.

[3] Zhou J, Di L, Cheng C, et al. A rotor unbalance response based approach to the identification of the closed-loop stiffness and damping coefficients of active magnetic bearings[J]. Mechanical Systems & Signal Processing, 2016, 66-67:665–678.

[4] Ma Y, He M, Shen W, et al. A planar shock isolation system with high-static-low-dynamic-stiffness characteristic based on cables[J]. Journal of Sound and Vibration, 2015, 358:267-284.

[5] Ma Y, Su Y, Yu S, Vibration Isolation of Rotating Machinery by Parameters Switched Magnetic Bearing and High Static Low Dynamic Stiffness Supports, presented at ASME Turbo Expo 2018, Lillestrøm (Oslo), Norway, 2018.

[6] Hu P, Ren G. Multibody dynamics of flexible liquid rockets with depleting propellant[J]. Journal of Guidance, Control, and Dynamics, 2013, 36:1840-1849.

[7] Zhao Z, Ren G. Multibody dynamic approach of flight dynamics and nonlinear aeroelasticity of flexible aircraft[J]. AIAA JOURNAL, 2011, 49:41-54.

[8] Zhao Z, Ren G. A quaternion-based formulation of Euler–Bernoulli beam without singularity[J]. Nonlinear Dynamics, 2012, 67:1825-1835.

[9] Krämer P D r n E. Dynamics of Rotors and Foundations[M]. Springer-Verlag, 1993.